



Comment on: "The spatial extent of the Deep Western Boundary Current into the Bounty Trough: new evidence from parasound sub-bottom profiling" by Horn and Uenzelmann-Neben

DOI:
[10.1007/s11001-016-9287-y](https://doi.org/10.1007/s11001-016-9287-y)

Document Version
Accepted author manuscript

[Link to publication record in Manchester Research Explorer](#)

Citation for published version (APA):

Mitchell, N. (2016). Comment on: "The spatial extent of the Deep Western Boundary Current into the Bounty Trough: new evidence from parasound sub-bottom profiling" by Horn and Uenzelmann-Neben. *Marine Geophysical Researches*, 37, 371-374. <https://doi.org/10.1007/s11001-016-9287-y>

Published in:
Marine Geophysical Researches

Citing this paper

Please note that where the full-text provided on Manchester Research Explorer is the Author Accepted Manuscript or Proof version this may differ from the final Published version. If citing, it is advised that you check and use the publisher's definitive version.

General rights

Copyright and moral rights for the publications made accessible in the Research Explorer are retained by the authors and/or other copyright owners and it is a condition of accessing publications that users recognise and abide by the legal requirements associated with these rights.

Takedown policy

If you believe that this document breaches copyright please refer to the University of Manchester's Takedown Procedures [<http://man.ac.uk/04Y6Bo>] or contact uml.scholarlycommunications@manchester.ac.uk providing relevant details, so we can investigate your claim.



1 Comment on: "The spatial extent of the Deep Western Boundary Current
2 into the Bounty Trough: new evidence from parasound sub-bottom
3 profiling" by Horn and Uenzelmann-Neben

4 Neil C. Mitchell

5 School of Earth, Atmospheric and Environmental Sciences, University of Manchester,
6 Williamson Building, Oxford Road, Manchester M13 9PL, UK.

7

8 Keywords: sediment profiler records, chirp records, Milankovic cycles

9

10 This is the green open-access version of this article:

11 Mitchell, N.C., Comment on: "The spatial extent of the Deep Western Boundary Current into
12 the Bounty Trough: new evidence from parasound sub-bottom profiling" by Horn and
13 Uenzelmann-Neben, Marine Geophysical Research, in press
14 (<https://link.springer.com/journal/11001>).

15

16

17 Horn and Uenzelmann-Neben (2016) have described computing power spectra from
18 sediment profiler data collected over the Bounty Trough from which they inferred
19 Milankovic cycles. Sediment profiler records are routinely acquired on research
20 vessels, so the method presented is interesting if it can help to resolve different
21 influences on sediment deposits from such data. A significant concern, however, is
22 that attenuation dominates the amplitude variation in profiler data, distorting power
23 spectra computed over the sediment age intervals of interest. In the case of the

24 Bounty Trough data shown, attenuation appears to have strongly varied amplitudes
25 over the depth range commensurate with the first 41 ky Milankovic cycle, so the
26 article's result is less certain than claimed. Attenuation rates can vary spatially (both
27 along track and with depth) so evaluating cycles will not be straightforward without
28 ground truth from boreholes, which potentially diminishes the utility of remote-
29 sensing data. Nevertheless, while not separating attenuation and reflectivity
30 unequivocally, alternative displays of such data as explained below can help to
31 suggest the relative importance of attenuation and reflectivity on amplitude variations.

32 The frequency analysis software of Schulz and Stattegger (1997) used by
33 Horn and Uenzelmann-Neben (2016) was originally designed to find periodic
34 variations in data series in the presence of noise. Aside from a single peak at ~14.5
35 m, the amplitudes shown in Figure 5a of Horn and Uenzelmann-Neben (2016)
36 decline sharply within the first 13 m below seabed. Amplitudes below 13 m are
37 generally less than 10% of the maximum amplitude. Figure 1 shows a compilation of
38 attenuation measurements, updated with data from Tyce (1981), who derived
39 sediment attenuation rates at 4 kHz (the frequency of the data of Horn and
40 Uenzelmann-Neben (2016)). He measured attenuation rates of 0.19 to 0.63 dB m⁻¹
41 in hemipelagic turbidites and other layered sediments broadly comparable with
42 those of the Bounty Trough. To illustrate how reflection data would be affected,
43 at 0.2 dB m⁻¹, a halving of amplitude (a change of 6 dB) occurs over 30 m. At 0.6
44 dB m⁻¹, a halving of amplitude would occur over 10 m. Given the decline in the
45 Bounty Trough data to only 10% of peak amplitude within 13 m, the attenuation
46 coefficient may be locally extreme, perhaps even >2 dB m⁻¹ (this is itself
47 interesting as such high attenuation rates at 4 kHz would commonly be
48 associated with sands, not the silty clays mainly found at Ocean Drilling Program

49 Site 1122 within the study area of Horn and Uenzelmann-Neben (2016), although
50 turbidites within these units contain some sand and the laminated structure may
51 cause unusually high transmission loss).

52 An effect of attenuation can be observed in Figure 2, which shows the average
53 of six traces of Chirp sediment profiler data collected in the central Red Sea (Mitchell
54 et al. 2015). These data were collected with a system with frequency swept over 2-7
55 kHz. They reveal prominent reflections in an area known to have climatically
56 modulated sediment properties (during sea level lowstands of the late Pleistocene, the
57 sea became more isolated and saline, leading to deposition of rigid aragonite-rich
58 layers (Gevirtz and Friedman 1966; Milliman et al. 1969; Stoffers and Ross
59 1974)). The pair of reflections within R1 was produced by the surface of the Last
60 Glacial Maximum sediments and by overlying Holocene sediments, while R2 to R5
61 represent reflections from deeper lowstand deposits.

62 The data have been plotted in Figure 2 with amplitude on a logarithmic scale.
63 Attenuation reduces amplitudes exponentially with propagation distance if attenuation
64 coefficient is uniform, so the logarithm of amplitude would be expected to be linear
65 with depth. Here, these data indeed show, below R1 (which has exaggerated
66 amplitudes because of contrast of sediments with low-impedance water), a systematic
67 variation with further two-way time. The straight dashed regression line fitted to the
68 data shown implies an attenuation coefficient of 0.34 dB m^{-1} , assuming sediment
69 velocity of 1500 m s^{-1} . This coefficient is potentially over-estimated because
70 progressive compaction with depth tends to reduce density and velocity contrasts
71 (reducing reflection amplitudes with depth), although 0.34 dB m^{-1} is compatible with
72 other attenuation data on similar sediments for this 2-7 kHz frequency band (Figure
73 1).

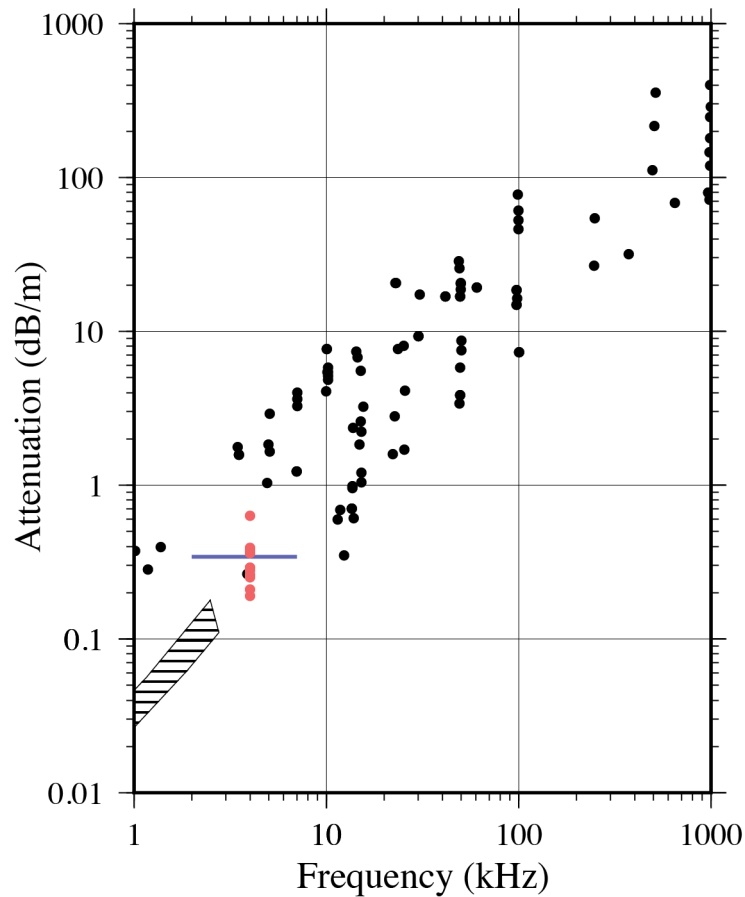
74 The red line in Figure 3 shows the amplitude data superimposed with the
75 attenuation trend (dashed red line). The blue line shows the effect of de-trending the
76 data using the regression line in Figure 2 and converting the logarithmic de-trended
77 data back into amplitudes. The principal trend in the red data is caused by the
78 attenuation, while the de-trended data have a more episodic variation more likely to
79 reveal periodicities if the data two-way times were transformed to sediment age. The
80 corresponding power spectra computed using the "spectrum1d" module of the Wessel
81 and Smith (1991) software shown in Figure 4 illustrate how dramatically spectra can
82 sometimes differ when computed with and without de-trending.

83 A preferable analysis procedure would therefore be to plot $\log(\text{amplitude})$
84 versus two-way time or depth. If such plots are linear, this may imply a uniform
85 attenuation rate, which can be evaluated against other attenuation measurements as
86 above. Even if plots are not linear, the attenuation component of any variation could
87 be assessed knowing the range of attenuation coefficients to be expected of the target
88 sediments. Where de-trending appears worthwhile, it also unfortunately enlarges
89 noise with increasing two-way travel time, which produces unwanted effects on
90 power spectra. However, noise effects could potentially be reduced by fitting periodic
91 functions to the data series (Fourier transforming) with weighting to account for
92 signal-to-noise ratio varying with two-way time. Interpreting sediment profiler
93 records in terms of Milankovic cycles is likely to be complicated, but the basic step of
94 plotting the data logarithmically as in Figure 2 may help to reveal whether variations
95 in profiler data along tracks are genuine variations in reflectivity or are artifacts of
96 varied attenuation.

97

98 **References**

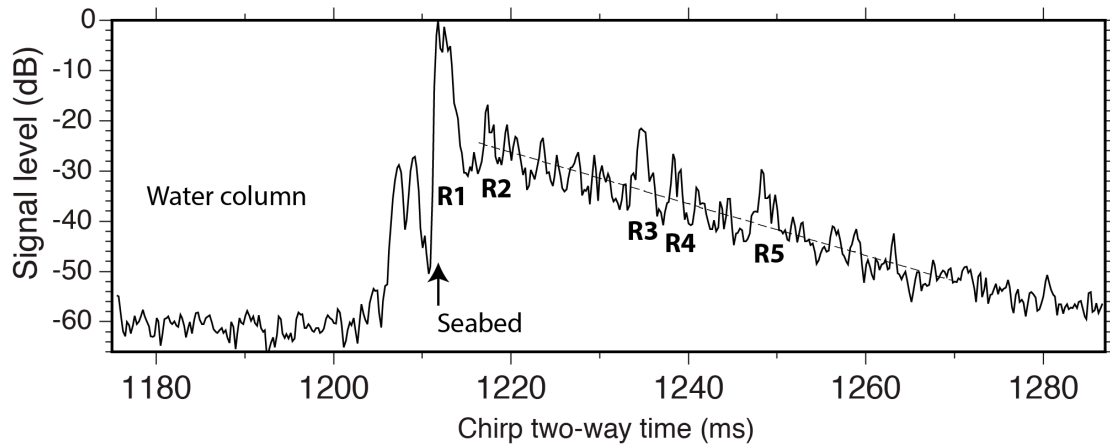
- 99 Gevirtz JL, Friedman GM (1966) Deep-sea carbonate sediments of the Red Sea and
100 their implications on marine lithification. *J. Sediment. Petrol.* 36:143-151
- 101 Hamilton EL (1980) Geoacoustic modeling of the sea floor. *J. Acoust. Soc. Am.*
102 68(5):1313-1340
- 103 Horn M, Uenzelmann-Neben G (2016) The spatial extent of the Deep Western
104 Boundary Current into the Bounty Trough: new evidence from parasound sub-
105 bottom profiling. *Mar. Geophys. Res.* 37:145-158
- 106 Milliman JD, Ross DA, Ku T-L (1969) Precipitation and lithification of deep-sea
107 carbonates in the Red Sea. *J. Sed. Petrol.* 39:724-736
- 108 Mitchell NC (1993) A model for attenuation of backscatter due to sediment
109 accumulations and its application to determine sediment thickness with GLORIA
110 sidescan sonar. *J. Geophys. Res.* 98:22477-22493
- 111 Mitchell NC, Ligi M, Rohling EJ (2015) Red Sea isolation history suggested by Plio-
112 Pleistocene seismic reflection sequences. *Earth Planet. Sci. Lett.* 430:387-397
- 113 Schulz M, Stattegger K (1997) Spectrum: spectral analysis of unevenly spaced
114 paleoclimatic time series. *Comput. Geosc.* 23:929-945
- 115 Stoffers P, Ross DA (1974) Sedimentary history of the Red Sea. in: Whitmarsh, R.B.,
116 O.E. Weser, D.A. Ross, et al., Initial reports of the Deep Sea Drilling Project U.S.
117 Government Printing Office 23:849-865
- 118 Tyce RC (1981) Estimating acoustic attenuation from a quantitative seismic profiler.
119 *Geophysics* 46(10):1364-1378
- 120 Wessel P, Smith WHF (1991) Free software helps map and display data. *Eos,*
121 *Transactions, American Geophysical Union* 72:441
- 122



123

124 Figure 1. Attenuation coefficients of marine sediments from Mitchell (1993), with
 125 data originally from Hamilton (1980). Attenuation values for finer grained
 126 sediments tend to be smaller and values for sand grade sediment higher at a given
 127 frequency. Blue bar represents attenuation coefficient of 0.34 dB m^{-1} over 2-7 kHz
 128 range for the Chirp data in Figure 2. Red circles represent attenuation measurements
 129 made by Tyce (1981) at 4 kHz using data collected with the Scripps Deep Tow over
 130 the Southern California Borderland (terrigenous sandy silt to clayey silt) and Rockall
 131 Trough (hemipelagic turbidites with silty clay with silt and sand layers).

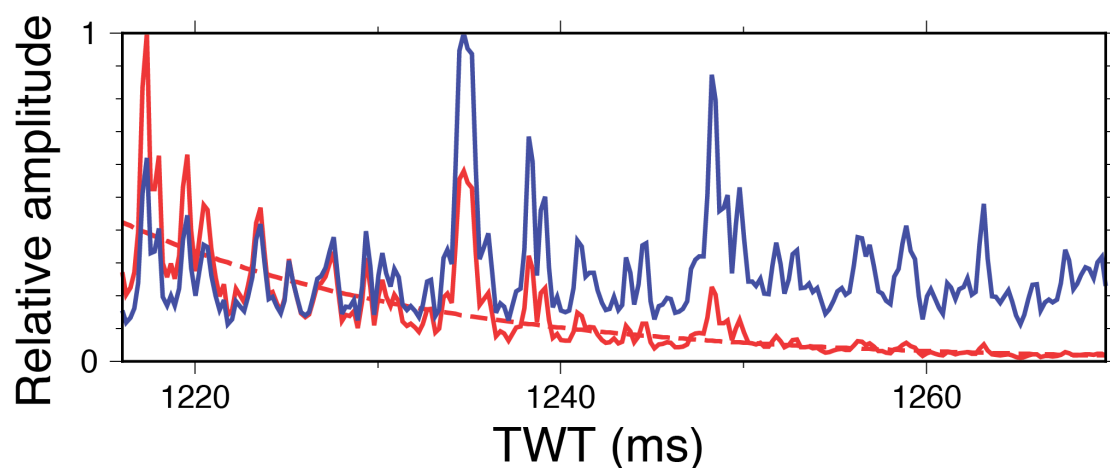
132



133

134 Figure 2. Chirp data amplitudes (average of 6 traces) collected in the central Red Sea
 135 (data corresponding to Figure 9 of Mitchell et al. (2015)). Amplitudes are plotted in
 136 decibels relative to the seabed reflection amplitude (i.e., $20\log_{10}(A/A_0)$, where A is the
 137 data amplitude and A_0 is the seabed reflection amplitude). Dashed line is simple least
 138 squares regression used to quantify the systematic trend in the data over the extent of
 139 two-way time covered by the dashed line. R1 to R5 are prominent reflections referred
 140 to in the text.

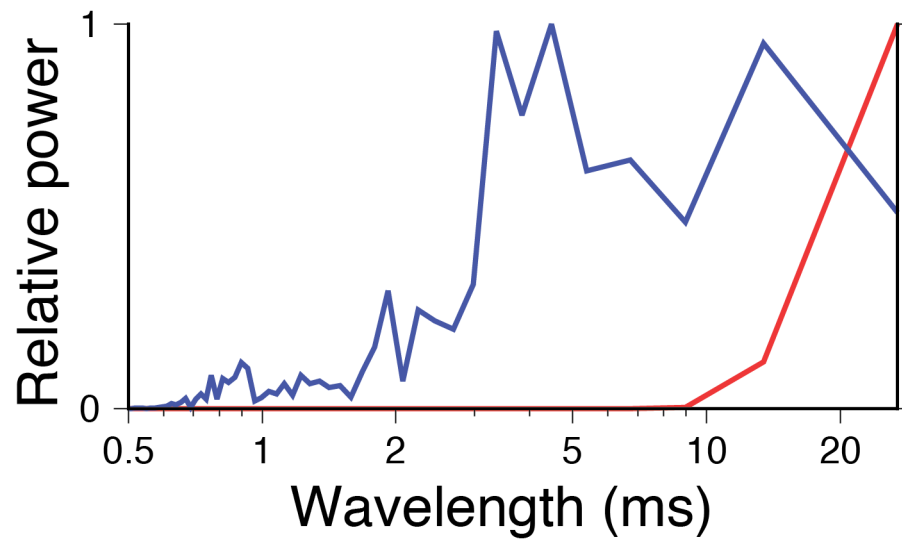
141



142

143 Figure 3. The data of Figure 2 plotted as linear amplitudes (red) and the result of de-
 144 trending (blue). Dashed red curve shows the regression line of Figure 2. Amplitudes
 145 are shown relative to maximum amplitude.

146



147

148 Figure 4. Power spectra computed from the data in Figure 3 (line colours correspond

149 with those in Figure 3).

150